Journal of Alloys and Compounds 509 (2011) 2364–2367

Contents lists available at ScienceDirect

Journal of Alloys and Compounds

journal homepage: www.elsevier.com/locate/jallcom

Effect of acetic acid complex on physical properties of nanostructured spray deposited $FeCdS_3$ thin films

A.U. Ubale*, S.G. Ibrahim

Thin Film Physics Laboratory, Department of Physics, Govt. Vidarbha Institute of Science and Humanities, VMV Road, Amravati 444604, Maharashtra, India

ARTICLE INFO

Article history:
Received 3 September 2010
Accepted 3 November 2010
Available online 10 November 2010

Keywords:
Nanostructures
Spray pyrolysis
Composite

ABSTRACT

Spray pyrolysis method which is simple as well as economic was used for the preparation of ternary nanostructured $FeCdS_3$ thin films onto glass substrates from ferric nitrate and cadmium chloride as Cd and Fe source and acetic acid as a complexing agent. The prepared films were characterized by X-ray diffraction (XRD), scanning electron microscopy (SEM) and optical absorption techniques. The structural, electrical, optical and morphological properties of $FeCdS_3$ thin films were influenced by quantity of acetic acid in spray solution. The X-ray spectrum and SEM reveal that the $FeCdS_3$ shows transition from nanocrystalline to amorphous phase depending on concentration of acetic acid. Optical band-gap of the amorphous and nanocrystalline film is found 2.40 and 2.65 eV, respectively. Nanocrystalline films have dark resistivity of the order of $10^3\ \Omega$ cm whereas amorphous films have $10^4\ \Omega$ cm. Thermoelectric power (TEP) measurement studies reveal that the films have p-type conductivity. It also shows that amorphous film generates less thermo-emf as compared to nanocrystalline film.

1. Introduction

Composite metal chalcogenide nanostructured thin films are attracting attention of research community because of their properties which are important in fabrication of various semiconductor devices. The energy gap can be engineered to cope up with the electromagnetic spectrum and therefore may be conveniently used in optoelectronic devices particularly in photoelectrochemical cells. In this regard iron pyrite (FeS_2) and cadmium sulfide (CdS) have attracted considerable attention as they posses potential candidature for photovoltaic and photo-electrochemical applications [1,2]. Ferrous sulfide belongs to VIII–VI compound semiconductor material of optical band gap 3 eV with high absorption coefficient of the order of $10^5\ cm^{-1}$ [3]. Several research reports are available concerning the preparation and properties of binary CdS and FeS_2 semiconductors. Liu et al. [4] have prepared pyrite films of thickness of 70–600 nm by annealing the iron films of thickness 25–150 nm at 673 K. The structural, optical and electrical characteristics were investigated and the effect of film thickness on properties was discussed. Dong et al. [5] have electrodeposited iron disulfide pyrite (FeS_2) thin films on indium doped tin oxide (ITO) substrates from aqueous solution containing $Na_2S_2O_3{\cdot}5H_2O$ and $FeCl_2{\cdot}4H_2O$ reagents. Yamamoto et al. [6] have used $FeSO_4$ and $(NH_4)_2S_x$ as precursors to deposit FeS_2 by spray method. Aqueous solutions of $FeSO_4$ and $(NH_4)_2S_x$ are sprayed alternately onto a substrate to get a p-type pyrite film containing no marcasite or pyrrhotite phase. Thomas et al. [7] have prepared cobalt doped pyrite films by indiffusion of a thin cobalt layer into a pyrite film deposited by metal organic chemical vapour deposition. Cobalt acts as a donor in pyrite and transforms the p-type conductivity into n-type. Pyrite (FeS_2) has been investigated as a potential absorber material for thin film solar cells [8–10] as it exhibits a very high absorption coefficient [11]. However, CdS thin films have been widely used as n-type semiconducting partners and buffer layers in electrochemical solar cells [12]. Hiie et al. [13] have prepared nanostructured CdS thin films by CBD and spray method using $CdCl_2$ and thiocarbamide as basic precursors and compared their electrical and optical properties. Ghosh et al. [14] have studied the effect of particle size and inter-electrode distance on the field-emission properties of nanocrystalline CdS thin films grown in a polymer matrix by chemical bath deposition method. Even though the several research reports are available on the preparation and properties of CdS and FeS_2 thin films, but very little is available on ternary $Cd_{1-x}Fe_xS$ [15,16]. Among various deposition techniques, spray paralysis methods is best suited for thin film deposition because of its simplicity to produce uniform, adherent and reproducible large area thin films for solar related applications. Hence, we have planned to carry out spray deposition of $FeCdS_3$ thin films and study their electrical, optical and structural properties. The efforts have been made to study the effect of complex acetic acid on properties of $FeCdS_3$ films deposited by the spray method.

* Corresponding author. Tel.: +91 721 2531706; fax: +91 721 2531705.
E-mail address: ashokuu@yahoo.com (A.U. Ubale).

0925-8388/$ – see front matter © 2010 Elsevier B.V. All rights reserved.
doi:10.1016/j.jallcom.2010.11.020

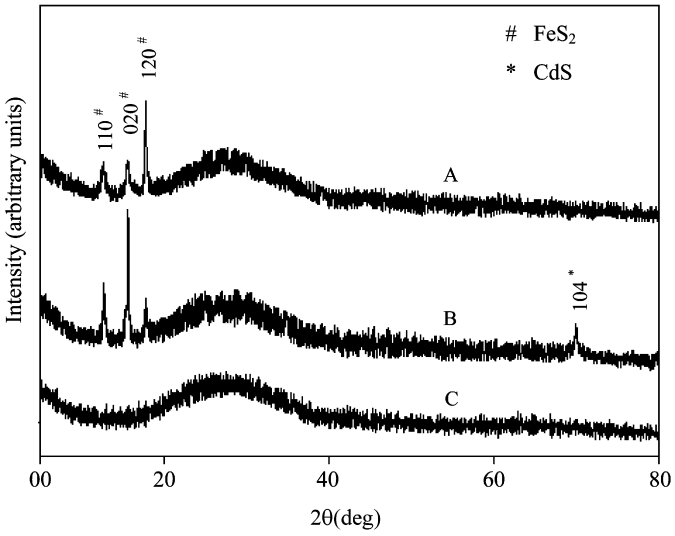

Fig. 1. XRD pattern of $FeCdS_3$ films deposited using acetic acid (A) 0.05 M, (B) 0.1 M and (C) 0.15 M.

2. Experimental details

Preparation of nanostructured ternary chalcogenide thin films can be easily achieved by spray pyrolysis method as it does not require sophisticated instruments. In present investigation for preparation of $FeCdS_3$ thin films 10 mL of ferric nitrate and cadmium chloride of concentration 0.1 M of each were mixed together to get transparent yellowish solution. In this solution, 10 mL acetic acid of concentration 0.05, 0.1 and 0.15 M was added separately to prepare three different spray configurations. Finally 10 mL of 0.1 M thiourea was mixed directly in each configuration to prepare spray solution. These solutions were sprayed onto hot glass substrates kept at 453 K using compressed air as a carrier gas at 6 cm^3 min^{-1} spray rate. The average thickness of the films was measured by the gravimetric and Fizzau's methods. Structural analysis was carried out using X-ray diffraction technique. Philips PW-1710 X-ray diffractometer with CuKα radiation (λ = 0.15405 nm) was used for phase identification, where diffracted X-ray intensities were recorded as a function of 2θ. The microstructure studies were carried out using JSM-6360 scanning electron microscope. The dark conductivity measurements were carried out by using the two-point probe method in the temperature range 309–423 K. Silver paste was applied to achieve ohmic contact with $FeCdS_3$ thin films. The type of conductivity of the film was determined by TEP measurement technique.

3. Result and discussion

In chemical spray pyrolysis method, the desired thin film material is obtained as a result of thermally activated reaction between the various species/complexes dissolved in the spray solution. During deposition process Fe^{3+} and Cd^{3+} cations and S^{2-} anions from the spray solution, react with each other to give neutral atoms by either spontaneously or very slowly on the hot substrate to produce $FeCdS_3$ depending upon the quantity of acetic acid in spray solution. In presence of acetic acid iron and cadmium ions forms acetate complex which decomposes rapidly to liberate Fe^{3+} and Cd^{3+} ions for the film formation. Ultimately the rate of decomposition was governed by the presence of acetic acid.

Fig. 1 shows the X-ray diffraction spectra of $FeCdS_3$ films. The XRD spectrum reveals that films deposited using 0.05 and 0.1 M acetic acid complex are nanocrystalline; whereas for higher concentration of acetic acid (0.15 M) the films are amorphous. Here at higher concentration of acetic acid, the cadmium and iron acetate species may undergo rapid thermal decomposition at hot substrate which produces random distribution of material on the substrate showing amorphous phase. At 0.05 M concentration of acetic acid XRD peaks are observed only due to orthorhombic phase of FeS_2. However, for 0.1 M acetic acid, a small additional peak due to hexagonal phase of CdS is observed. The comparison of observed and standard data for $FeCdS_3$ is given in Table 2. The grain size of crystallites was calculated by using Scherrer formula,

$$d = \frac{\lambda}{\beta \cos \theta} \quad (1)$$

where λ is the wavelength used (0.154 nm); β is the angular line width at half maximum intensity; θ is the Bragg's angle. The grain size of the film deposited using 0.05 M acetic acid is of the order of 9 nm and it increases to 11 nm for 0.1 M acetic acid.

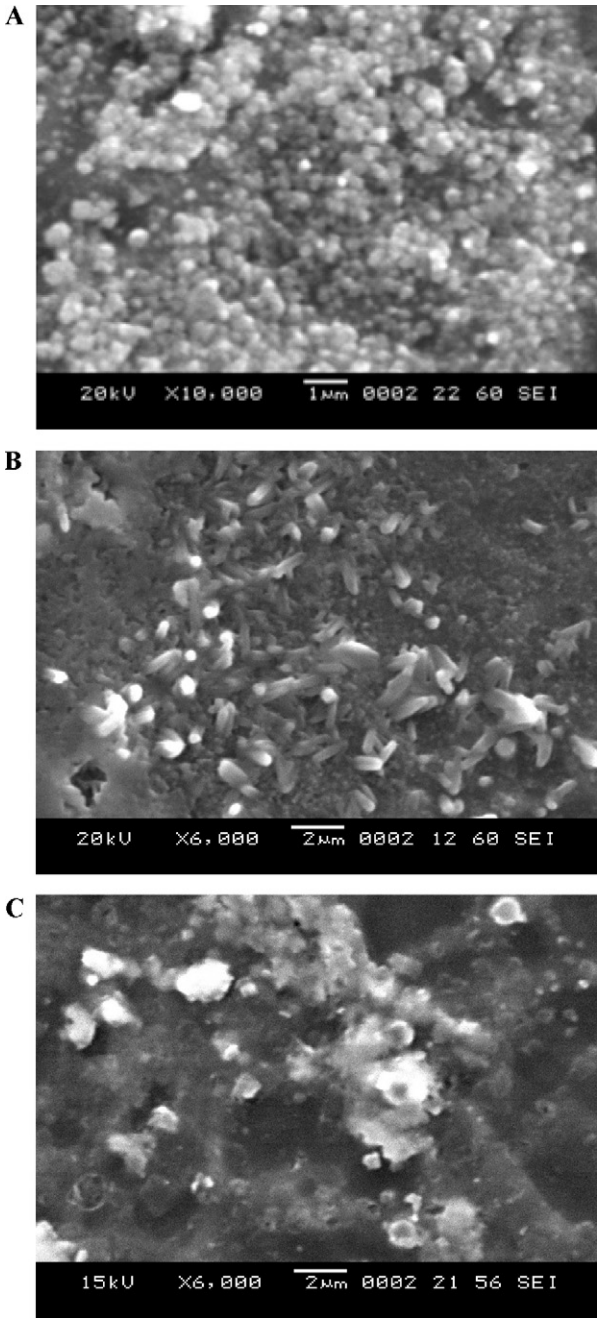

Fig. 2. SEM images of $FeCdS_3$ films: deposited using acetic acid (A) 0.05 M, (B) 0.1 M and (C) 0.15 M.

The SEM micrographs of $FeCdS_3$ films are shown in Fig. 2. The film deposited from 0.05 M acetic acid shows porous surface with circular nano-grains throughout the film surface. At 0.1 M concentration of acetic acid SEM image shows enhanced grain growth with rod-like structure. However, for higher concentration of acetic acid the film surface shows uniform distribution of amorphous phase of $FeCdS_3$ without cracks covering entire substrate surface area.

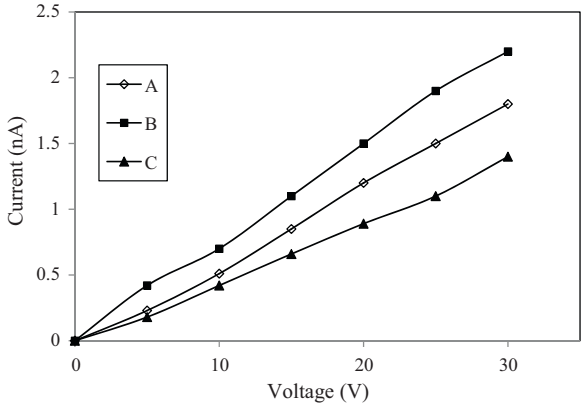

Fig. 3. *I–V* characteristic of $FeCdS_3$ films: deposited using acetic acid (A) 0.05 M, (B) 0.1 M and (C) 0.15 M.

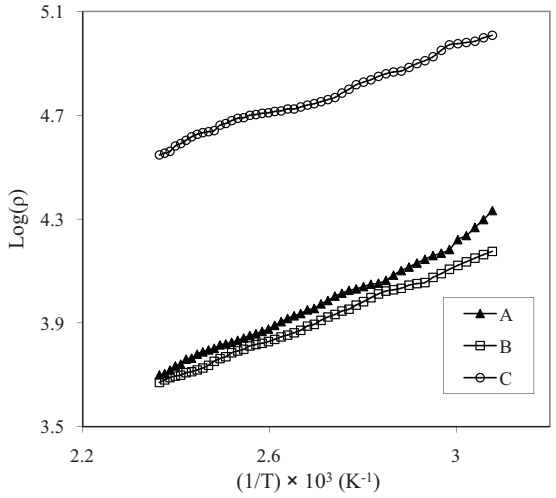

Fig. 4. Variation of Log of resistivity with $1/T$ for $FeCdS_3$ films: deposited using acetic acid (A) 0.05 M, (B) 0.1 M and (C) 0.15 M.

The *I–V* characteristics of $FeCdS_3$/Ag contacts were studied in order to check the nature of the contact. Fig. 3 shows that *I–V* characteristics of films are linear which confirms that silver produces ohmic contact with $FeCdS_3$. Fig. 4 shows variation of DC-electrical resistivity with temperature in the temperature range of 309–423 K. It was observed that resistivity decreases as the film temperature increases which confirms semiconducting nature of $FeCdS_3$. The resistivity of the film deposited using 0.05 M acetic acid is $5 \times 10^3\ \Omega$ cm at 413 K and it decreases slightly for the film deposited from 0.1 M acetic acid and then rises to $35.27 \times 10^3\ \Omega$ cm for 0.15 M acetic acid (Table 1). The change in resistivity may be due to the change in grain structure with concentration of acetic acid as seen in SEM images. The thermal activation energy of $FeCdS_3$ was calculated by using the relation,

$$\rho = \rho_0 \exp\left(\frac{E_0}{KT}\right) \quad (2)$$

Table 2
Comparison of observed and standard XRD data for $FeCdS_3$ films.

Sample	Observed		Standard JCPDS data for FeS_2 and CdS		
	2θ (°)	d (Å)	2θ (°)	d (Å)	$h\,k\,l$
A	11.822	3.421	11.835	3.440	1 1 0
	15.723	2.719	15.039	2.710	0 2 0
	17.543	2.327	17.586	2.320	1 2 0
B	11.825	3.432	11.835	3.440	1 1 0
	15.069	2.720	15.039	2.710	0 2 0
	17.526	2.331	17.586	2.320	1 2 0
	60.982	1.500	60.912	1.5197	1 0 4

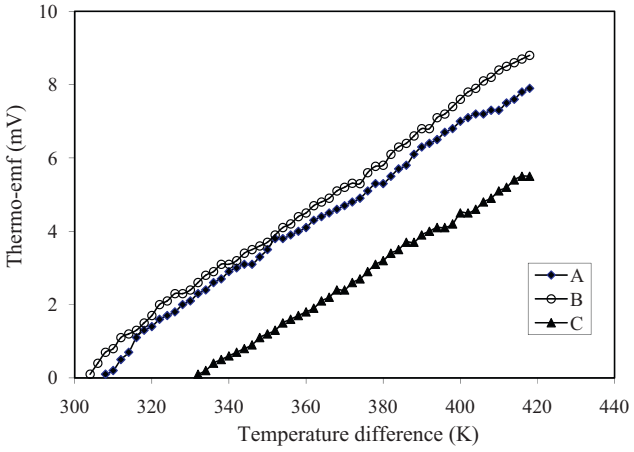

Fig. 5. Variation of thermo emf (mV) with temperature difference for $FeCdS_3$ films deposited using acetic acid (A) 0.05 M, (B) 0.1 M and (C) 0.15 M.

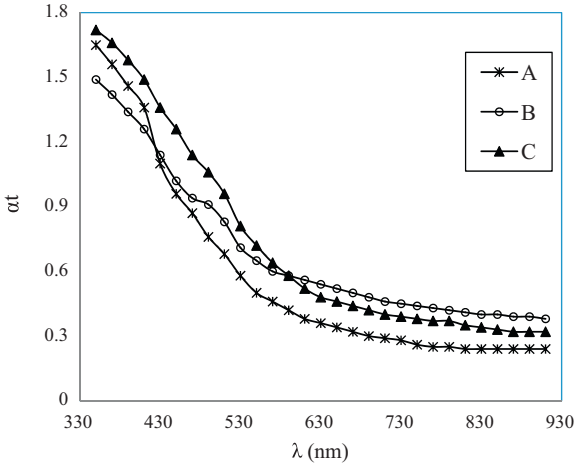

Fig. 6. Variation of optical absorption vs. wavelength of $FeCdS_3$ films: deposited using acetic acid (A) 0.05 M, (B) 0.1 M and (C) 0.15 M.

where ρ is resistivity at temperature T, ρ_0 is a constant; K is Boltzmann constant. The activation energy determined is of the order of ~0.1 eV for $FeCdS_3$ (Table 1).

The TEP of $FeCdS_3$ films was measured as a function of temperature in dark in the temperature range of 304–418 K (Fig. 5). The

Table 1
Band-gap energy, activation energy and resistivity of $FeCdS_3$.

Sample	Acetic acid concentration (M)	Film thickness (nm)	Band-gap energy (eV)	Activation energy (eV)	Resistivity at 423 K ($\times 10^3\ \Omega$ cm)
A	0.05	143	2.65	0.14	5.00
B	0.10	136	2.45	0.12	4.68
C	0.15	141	2.40	0.15	35.27

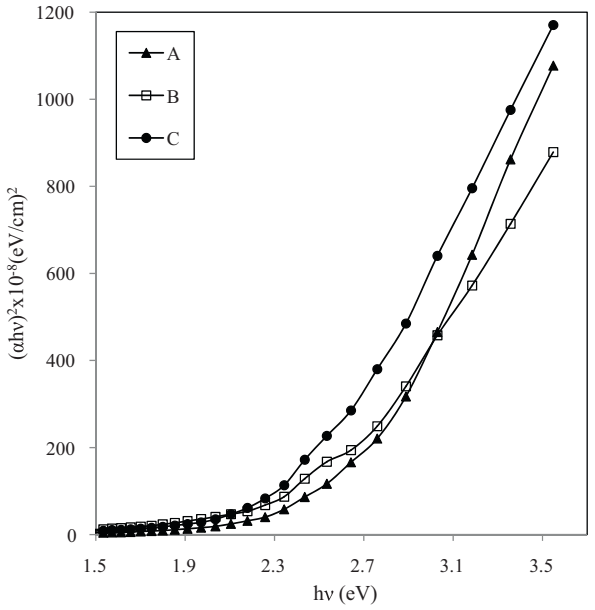

Fig. 7. Plots of $(\alpha h\nu)^2$ vs. $h\nu$ of $FeCdS_3$ films: deposited using acetic acid (A) 0.05 M, (B) 0.1 M and (C) 0.15 M.

polarity of the thermo-emf confirms n-type conductivity of $FeCdS_3$. The generated thermo-emf is more for the film deposited form 0.05 and 0.1 M acetic acid than the film deposited from 0.15 M acetic acid as the crystalline nature of film decreases for higher concentration of acetic acid.

Fig. 6 shows the variation of optical absorption of $FeCdS_3$ film in the wavelength range of 350–910 nm. The absorption spectra is analysed to find band-gap energy of $FeCdS_3$. The nature of the transitions involved can be determined on the basis of the dependence of the absorption coefficient, α or a multiple of it on $h\nu$. The nature of transition is determined by using the relation,

$$\alpha = \frac{A(h\nu - E_g)^n}{h\nu} \quad (3)$$

where $h\nu$ is the photon energy, E_g is the band-gap energy, A and n are constants. For the allowed direct transitions, $n = 1/2$ and for allowed indirect transitions $n = 2$. The optical energy gap E_g could be obtained from the plot of $(\alpha h\nu)^2$ versus $h\nu$ for direct allowed transitions. The $(\alpha h\nu)^2$ versus $h\nu$ plots for $FeCdS_3$ thin films deposited from 0.05, 0.1 and 0.15 acetic acid are presented in Fig. 7. The optical band-gap was shifted from 2.40 eV to 2.65 eV depending on acetic acid content in the spray solution. This shift in band-gap energy values can be explained on the basis of different size effects such as quantum size effect arising in the nanostructured films [17,18].

4. Conclusions

Nanostructured $FeCdS_3$ thin films were successfully prepared by chemical spray pyrolysis technique. The effect of complexing agent acetic acid on structural, electrical and optical properties of nanostructured $FeCdS_3$ films was studied. The X-ray diffraction pattern shows that the films deposited below 0.15 M concentration of acetic acid are nanocrystalline. Optical band-gap of the amorphous film is found 2.40 eV; where as it was 2.65 eV for the nanocrystalline film. The electrical characterizations were carried out by measuring resistivity and TEP of $FeCdS_3$ films deposited using various concentrations of acetic acid.

Acknowledgement

The authors are thankful to University Grants Commission, WRO, Pune (India), for financial support under the project (No. F47-258/2007).

References

[1] M. Ristov, Sol. Energy Mater. Sol. Cells 53 (1998) 95.
[2] D. Behar, I. Rubinstein, G. Hodes, Superlat. Microstruct. 25 (1999) 601.
[3] H.M. Pathan, C.D. Lokhande, Bull. Mater. Sci. 27 (2004) 85.
[4] Y.H. Liu, L. Meng, L. Zhang, Thin Solid Films 479 (2005) 83.
[5] Y.Z. Dong, Y.F. Zheng, H. Duan, Y.F. Sun, Y.H. Chen, Mater. Lett. 59 (2005) 2398.
[6] A. Yamamoto, M. Nakamura, A. Seki, E.L. Li, A. Hashimoto, S. Nakamura, Sol. Energy Mater. Sol. Cells 75 (2003) 451–456.
[7] B. Thomas, K. Ellmer, W. Bohne, J. Rohrich, M. Kunst, H. Tributsch, Solid State Commun. 111 (1999) 235.
[8] W. Jaegermann, H. Tributsch, J. Appl. Electrochem. 13 (1983) 743.
[9] A. Ennaoui, H. Tributsch, Sol. Cells 13 (1984) 197.
[10] A. Ennaoui, S. Fiechter, C. Pettenkofer, N. Alonso-Vante, K. Buker, M. Bronold, C. Hopfner, H. Tributsch, Sol. Energy Mater. Sol. Cells 29 (1993) 289.
[11] I.J. Ferrer, D.M. Nevskaia, C. de las Heras, C. Sanchez, Solid State Commun. 74 (1990) 913.
[12] D. Bonnet, Proc. of 19th European PV Solar Energy Conf., vol. 2, WIP-Munich and ETA – Florence, 2004, p. 1657.
[13] J. Hiie, T. Dedova, V. Valdna, K. Muska, Thin Solid Films 511/512 (2006) 443.
[14] P.K. Ghosh, S. Jana, U.N. Maity, K.K. Chattopadhyay, Physica E 35 (2006) 178.
[15] N. Badera, B. Godbole, S.B. Srivastava, P.N. Vishwakarma, L.S. Sharath, Appl. Surf. Sci. 254 (2008) 7042.
[16] K.W. Liu, J.Y. Zhang, D.Z. Shen, B.H. Li, X.J. Wu, B.S. Li, Y.M. Lu, X.W. Fan, Thin Solid Films 515 (2007) 8017.
[17] A.U. Ubale, D.K. Kulkarni, Bull. Mater. Sci. 28 (1) (2005) 43.
[18] A.U. Ubale, D.K. Kulkarni, Ind. J. Pure Appl. Phys. 44 (2006) 254.